2013

Magnetic hollow cages with colossal moments

Menghao Wu
Virginia Commonwealth University

Puru Jena
Virginia Commonwealth University, pjena@vcu.edu

Wu, M., and Jena, P. Magnetic hollow cages with colossal moments. The Journal of Chemical Physics, 139, 044301 (2013).

Magnetic hollow cages with colossal moments

Menghao Wu and Puru Jena[a)]
Physics Department, Virginia Commonwealth University, Richmond, Virginia 23284, USA

(Received 8 April 2013; accepted 14 June 2013; published online 22 July 2013)

A comprehensive study of the interaction of transition metal clusters with B, C, N, O, and Si reveal novel structure and properties: $Co_{12}C_6$, $Mn_{12}C_6$, and $Mn_{24}C_{18}$ clusters form stable ferromagnetic hollow cages with total magnetic moments of 14 μ_B, 38 μ_B, and 70 μ_B, respectively. Replacement of C with B, N, O, or Si has significant impact on their structure and magnetic properties. For example, $Mn_{20}Si_{12}$ cluster forms a ferrimagnetic dodecahedral hollow cage with a total magnetic moment of 36 μ_B while $Mn_{12}N_6$, $X_{12}C_6$ (X = Ni, Cu, Pd, Pt), and $Cu_{12}O_6$ possess no magnetic moment, although they retain hollow cage structures. $Mn_{12}B_6$ and $Mn_{24}Si_{18}$, on the other hand, form compact ferrimagnetic structures. Synthesis of hollow cage clusters with unique magnetic properties may lead to important applications. © *2013 AIP Publishing LLC*. [http://dx.doi.org/10.1063/1.4813022]

INTRODUCTION

The discovery of C_{60} fullerene[1] with hollow cage structure has stimulated considerable interest in the search for similar clusters involving other elements. One of the reasons for this interest is that hollow cage clusters with embedded atoms or molecules may have technological applications. Unfortunately, this search has met with little success in metal clusters which usually form compact geometries. Metallorcarbohedrenes (commonly known as Met-Cars) consisting of 8 transition metal atoms (V, Zr, Hf, Ti, Nb, Mo, Fe, or Cr) and 12 carbon atoms [2–10] were initially thought to form pentagonal dodecahedral hollow cage structures, but later studies showed that the ground state geometries of Met-cars are not hollow cages and compact isomers have lower energies.[11,12] At present, a few hollow metal cage structures like Sn_{10}^{2-}, Pb_{10}^{2-},[13,14] Au_{16}^{-}, Au_{18}^{-} anions,[15] and metal oxide cages[16] have been confirmed in experiment, and some bimetallic cages have been predicted recently,[17] but they all have small hollow space and small magnetic moments, if any.

In this paper, we propose a new type of compound metal clusters that simultaneously form hollow cages and carry giant magnetic moments. We first focus on clusters composed of Mn and C. Unlike Met-Cars which are carbon rich, our systems contain less number of carbon atoms than metal atoms. Our choice of Mn as the metal atom is primarily dictated by its unique properties. Due to its half-filled 3*d* and a filled 4*s* shell ($3d^5\ 4s^2$) Mn atoms do not interact strongly with each other and bulk Mn has the lowest cohesive energy (2.9 eV/atom) among all 3*d*-transition metals. The oxidation state of Mn can vary from 0 to +7, although it is predominantly divalent. Because of this Mn atoms often retain a magnetic moment of 5 μ_B when forming compounds. While bulk Mn is antiferromagnetic, it has been demonstrated both theoretically and experimentally that small Mn clusters containing less than five atoms are ferromagnetic.[18–25] If these atoms could couple ferromagnetically in larger sizes, a cluster of *n* Mn atoms could carry a magnetic moment of $5n\ \mu_B$. Unfortunately, Mn clusters consisting of more than 5 atoms carry small net magnetic moments.[21–25] For example, Mn_{13} cluster with a preferred icosahedric structure has magnetic moment of only 3 μ_B. However, the coupling in Mn_{13} changes to ferromagentic with a net magnetic moment of 47 μ_B when the cluster assumes a cuboctahedric structure.[26] This structure, however, is unstable and is almost 3 eV higher in energy than the icosahedric structure. The magnetic coupling between the Mn atoms is very sensitive to their interatomic distance as was shown to be the case by a detailed study of the Mn_2 dimer.[27] In addition, it was shown[28] nearly a decade ago that Mn clusters containing up to five atoms, when doped with a N atom, can become ferromagnetic with Mn_5N carrying a total magnetic moment of 22 μ_B. A recent study of $Mn_{13}N$, however, revealed it to be ferrimagnetic with a net magnetic moment of only 12 μ_B.[29] We have recently shown that Mn_{13} can become ferromagnetic by doping five or six carbon or boron atoms.[30] Another Mn cluster that was predicted to have a high spin state of 44 μ_B is $Mn_{13}Au_{20}^{-}$ *anion,* although a low spin state (2 μ_B) is only 0.07 eV higher in energy.[31] None of these clusters form hollow cage structures.

The above studies indicate that it may be possible to tailor the magnetic coupling between Mn atoms by manipulating their interatomic distance either by doping or by fixing their charge state. Consequently, we have carried out a comprehensive study of the electronic structure and magnetic properties of Mn clusters with varying size and by doping them with B, C, N, O, and Si. We find that *neutral* $Mn_{12}C_6$, with only six carbon atoms, is not only ferromagnetic with a magnetic moment of 38 μ_B but also it forms a hollow cage structure initially envisioned for Met-Cars. Furthermore, the magnetic moment can be substantially enhanced by nearly doubling its size: $Mn_{24}C_{18}$ forms a ferromagnetic hollow cage structure larger than C_{60} with a magnetic moment of 70 μ_B! Calculations were also carried out by replacing Mn with other 3*d*-transition metal elements such as Sc, Ti, V, Fe, Co, Ni, and Cu.

a)Email: pjena@vcu.edu

COMUTATIONAL PROCEDURE

The equilibrium structures, total energies, and magnetic properties of various isomers of compound clusters mentioned in the above are calculated using the DMol^3 4.1 package.[32,33] The generalized gradient approximation (GGA) for the exchange-correlation potential prescribed by Perdew-Burke-Ernzerhof (PBE) and an all-electron double numerical basis set (DNP) with polarization functions are used in spin-unrestricted density-functional-theory (DFT) based calculations.[34] We note that the DFT-PBE level of theory has been used in the past[24,35] to calculate the magnetic moments of Fe_n (n = 12, 13, 14) and Mn_n (n = 5∼20) clusters and the results agree very well with available experimental data. The real-space global cutoff radius is set at 4.7 Å. After optimization, the forces on all atoms are less than 0.0002 Ha/Å. For clusters containing Ag or Au atoms, relativistic all-electron DFT calculations are performed. To complement the DMol^3 results, we have used the Vienna *ab initio* Simulation Package (VASP)[38–40] to calculate the energies as a function of total magnetic moment for all possible configurations. In both cases, we used the DFT-PBE level of theory. Note that in DMol^3, the atomic basis sets are numerical functions on an atom-centered grid while VASP uses projector augmented-wave pseudopotentials method.[36,37]

The most important step in the calculation is to obtain the geometry of a cluster corresponding to its global minimum in the energy landscape. This is indeed a very difficult task at the first principles level of theory as there are numerous local minima whose number increase exponentially as the number of atoms in the cluster increases. While several search procedures such as basin hopping and genetic algorithm are available, one is never sure that lowest energy structure has been reached. We have, therefore, started our optimization procedure by using several initial configurations where the dopant atoms are placed either separately or in groups in various locations of the parent metal cluster. Our searches are not constrained by symmetry and the clusters have the freedom to sample the phase space. The stability of the cluster with the lowest energy was further validated by carrying out *ab initio* molecular dynamics simulation.

RESULTS AND DISCUSSIONS

We begin with the geometry of the lowest energy structure of $Mn_{12}C_6$. The various initial structures used in the geometry optimization are given in Fig. S1 of the supplementary material.[41] These configurations included the ground state of the Mn_{12} cluster determined previously by other authors. The energies of these structures were found to be larger than that obtained by decorating the cuboctahedral (Oh) Mn_{12} hollow shell with six C atoms. We note that the cuboctahedral (Oh) structure has eight triangular faces and six square faces. If we consider that the bond length of Mn-Mn should vary from 2.5 to 2.8 Å as has been seen to be the case from earlier studies of pure Mn clusters, then for every Mn square face, the distance from center of the square to Mn atom would vary from 1.8 to 2.0 Å. Since the bond length of C-Mn is around 2.0 Å, we placed each C atom at the center of every square face and

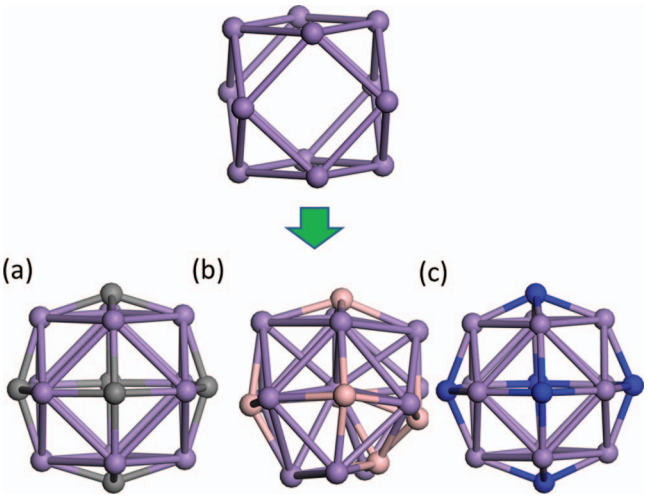

FIG. 1. Geometrical structures of ground-state (a) $Mn_{12}C_6$, (b) $Mn_{12}B_6$, and (c) $Mn_{12}N_6$ clusters. Purple, pink, gray, and blue spheres denote Mn, B, C, and N atoms, respectively.

optimized the structure of $Mn_{12}C_6$ without imposing any symmetry constraint. Upon optimization, this resulted in a hollow cage structure (H structure) shown in Fig. 1(a). Here the C atoms are all displaced slightly from the center of the square faces and become respectively quasi-planar. Every Mn atom has four Mn-Mn bonds and two Mn-C bonds and $Mn_{12}C_6$ has a slightly distorted Oh symmetry. Simulated annealing for 10 ps with a time step of 1.5 fs was carried out by gradually reducing the temperature from 900 to 0 K. The final configuration was found to retain the hollow cage structure. Vibrational analysis yielded no imaginary frequencies and the lowest vibrational frequency is 91.3 cm^{-1}. These studies confirm that the hollow cage structure of $Mn_{12}C_6$ is indeed stable. Equally important, $Mn_{12}C_6$ is found to be ferromagnetic with a giant magnetic moment of 38 μ_B. Since the empty space in the center of the cage is large enough to accommodate a Mn atom, we considered another isomer of $Mn_{12}C_6$ by moving one Mn atom from the surface to the center. We denote this structure as the "filled" structure (F structure). We found the hollow cage structure of $Mn_{12}C_6$ to be 0.72 eV lower than the filled structure.

To verify the accuracy of the above result obtained from Dmol^3, we calculated the total energies of $Mn_{12}C_6$ clusters for different spin states by using the VASP code. The results are plotted in Figure 2. Here we find that the magnetic moments of these clusters in the ground state obtained using both DMol^3 and VASP are the same. We also find that for $Mn_{12}C_6$, the low spin states are in general much higher in energy than the ground state, suggesting that the high spin state is indeed very stable. The spin density distribution of the ground-state structures of $Mn_{12}C_6$ in Fig. 3(a) confirms ferromagnetic ordering.

As mentioned in the above, the space inside $Mn_{12}C_6$ cage is large enough to accommodate only a single atom and does not allow the flexibility of incorporating molecules or larger clusters. We wondered if metal hollow cages as large as C_{60} can possibly exist. We recall that the key to stabilize the hollow cage studied in the above is to place carbon atoms at the

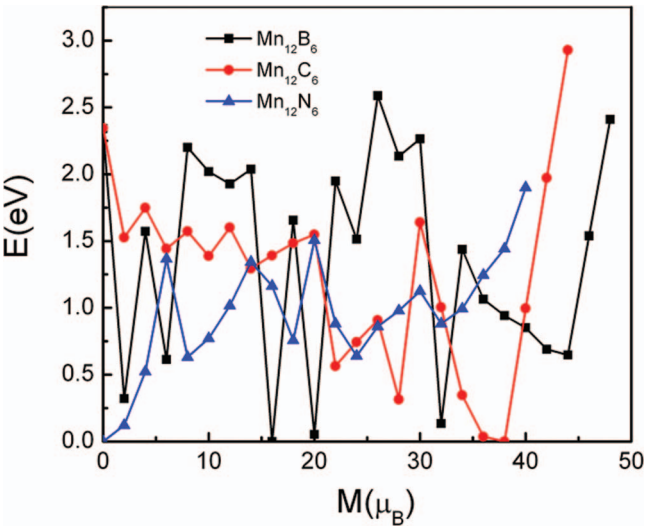

FIG. 2. Relative energies of $Mn_{12}C_6$, $Mn_{12}B_6$, and $Mn_{12}N_6$ in different spin states with respect to the lowest-energy states.

center of square faces. Consequently, we looked for structures containing larger number of square faces. One such structure is a rhombicuboctahedron which has 24 identical vertices, eight triangular, and 18 square faces. When the 24 vertices are occupied by Mn atoms and a C atom is placed at the center of every square face, the resulting structure yields a $Mn_{24}C_{18}$ cluster. Upon structure optimization, $Mn_{24}C_{18}$ is indeed found to have a hollow structure shown in Fig. 4(a). This hollow cage is so large that it can even accommodate the whole $Mn_{12}C_6$ cluster in it. The average Mn-Mn bond length here is 2.60 Å, almost same as that in $Mn_{12}C_6$. As a result the system is ferromagnetic and has a magnetic moment of 70 μ_B. To complement the results based on Dmol[3], we calculated the total energies of $Mn_{24}C_{18}$ for different spin states by using the plane wave electronic structure code, VASP. The results are

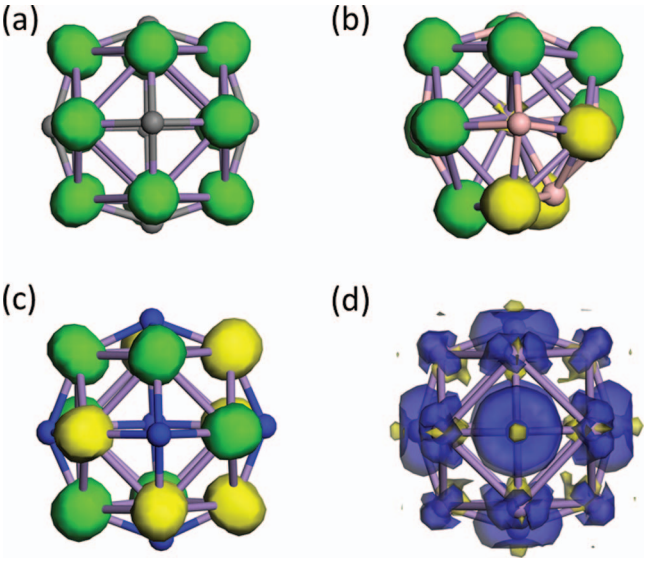

FIG. 3. Spin density distribution of the ground-state of (a) $Mn_{12}C_6$, (b) $Mn_{12}B_6$, and (c) $Mn_{12}N_6$. (d) is deformation density distribution of $Mn_{12}C_6$. In (a–c), green and yellow denote spin-up and spin-down densities, respectively, and iso-values of spin density range from −0.5 to 0.5.

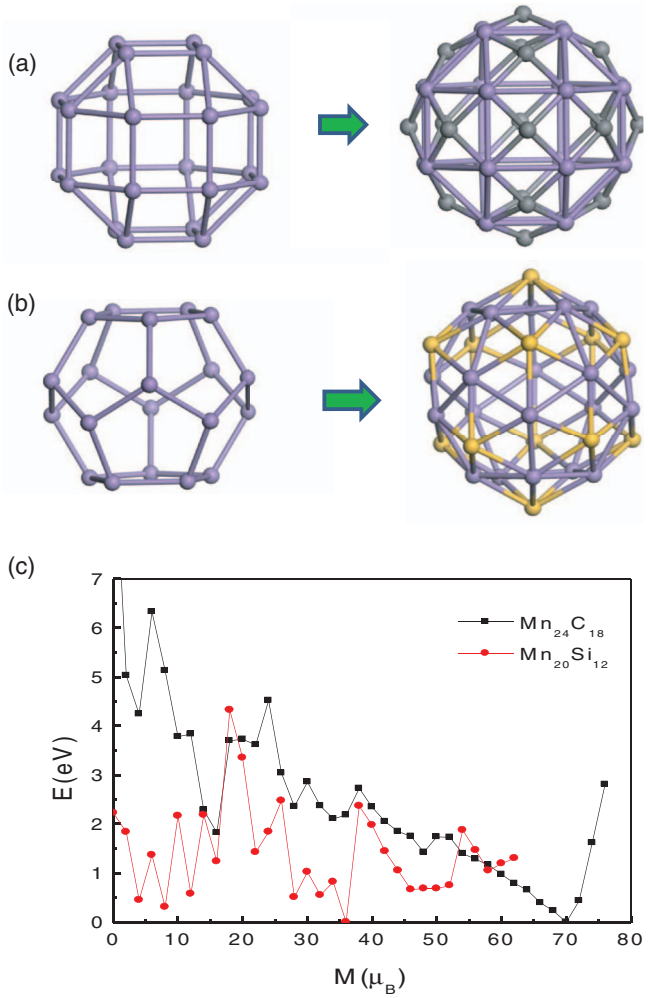

FIG. 4. Geometric structures of (a) $Mn_{24}C_{18}$, (b) $Mn_{20}Si_{12}$, and (c) their relative energies in different spin states with respect to the lowest-energy states.

plotted in Figure 4(c). We again find the magnetic moments of these clusters in the ground state obtained using both DMol[3] and VASP to be the same. Vibrational analysis yielded no imaginary frequencies, and the lowest vibrational frequency, namely, 98.9 cm^{-1} is even higher than that of $Mn_{12}C_6$. This suggests that the $Mn_{24}C_{18}$ hollow cage could be even more stable than $Mn_{12}C_6$. This is understandable since every Mn atom here has four Mn-Mn bonds and three Mn-C bonds. Thus, it has one more Mn-C bond than that in $Mn_{12}C_6$. The total energy of $Mn_{24}C_{18}$ hollow cage cluster was compared with a number of other isomers which are all much higher in energy, as shown in Figs. S2(a)–S2(e)[41] of the supplementary material. The binding energy with respect to dissociation of $Mn_{24}C_{18}$ into Mn_{24} and C_{18} cluster is 18.7 eV.

We studied the effect of replacing the C atoms with B and N atoms on the equilibrium geometries and magnetic properties of $Mn_{12}B_6$ and $Mn_{12}N_6$ clusters. Since Mn-B and Mn-N bond distances are also around 2 Å, we first determined the equilibrium geometries of $Mn_{12}B_6$ and $Mn_{12}N_6$ clusters by optimizing their geometries in a manner similar to that done for $Mn_{12}C_6$. The results are shown in Figs. 1(b) and 1(c). We find that $Mn_{12}B_6$ prefers a distorted filled structure (the hollow cage isomer is 2.0 eV higher in energy), while $Mn_{12}N_6$

prefers the hollow cage structure (the corresponding filled isomer is 0.95 eV higher in energy) with C2 symmetry. This difference in the ground state geometries between $Mn_{12}B_6$ and $Mn_{12}C_6$ as well as $Mn_{12}N_6$ persists even if we force $Mn_{12}B_6$ to assume a ferromagnetic state; $Mn_{12}B_6$ still prefers a distorted filled structure (the hollow cage isomer is 1.35 eV higher in energy), while $Mn_{12}N_6$ prefers the hollow cage structure (the corresponding filled isomer is 0.44 eV higher in energy).

All N atoms are displaced slightly from the center of the square faces and become tetrahedrally coordinated to Mn. Vibrational analysis yielded no imaginary frequencies and the lowest vibrational frequency of $Mn_{12}N_6$ is 91.3 cm^{-1}. This confirms that the hollow cage structure of $Mn_{12}N_6$ is stable. The magnetic moments of $Mn_{12}B_6$ and $Mn_{12}N_6$ are 16 and 0 μ_B, respectively, i.e., $Mn_{12}B_6$ is ferrimagnetic with the spins of eight Mn atoms aligned antiparallel to the spins of the other four atoms. $Mn_{12}N_6$, on the other hand, is antiferromagnetic with six Mn atoms aligned antiparallel to the spins of the other six atoms. These spin density distributions plotted in Figs. 3(b) and 3(c) are consistent with the calculated magnetic moments. For $Mn_{12}N_6$, we also calculated several noncollinear spin structures and they are all higher in energy than collinear one in ground state. These results are given in the supplementary material (see Fig. S3).[41]

The origin of the different structures when Mn_{12} is doped with six B, N, or C atoms can be traced to their electronegativity. We note that B is not as electronegative as C or N. Thus, B-Mn bond is weaker than those of C–Mn or N–Mn bonds. Consequently, it is energetically not favorable for the central Mn atom with eleven Mn-Mn bonds to move out to the shell to bind with more B atoms. Hence, the compact filled structure $Mn_{12}B_6$ is more stable than the hollow structure. This is also consistent with their binding energies with respect to dissociation of $Mn_{12}B_6$ into Mn_{12} and B_6 or $Mn_{12}C_6$ into Mn_{12} and C_6 clusters. These values are 11.3 eV for $Mn_{12}B_6$ and 12.1 eV for $Mn_{12}C_6$.

In Table I, we list the HOMO-LUMO gaps, the average charge on Mn in pure and doped clusters computed by the Hirshfeld method, the average Mn-Mn bond length, the total magnetic moment, and the average value of the local magnetic moment of Mn in the ground state of $Mn_{12}B_6$, $Mn_{12}C_6$, and $Mn_{12}N_6$ clusters. In previous work HOMO-LUMO gaps computed by using PBE for neutral clusters were found to be in good agreement with data obtained in vertical photodetachment experiments.[42] The HOMO-LUMO gaps of these clusters are much larger than that of Met-cars, namely, 0.096 eV for Ti_8C_{12}.[11] Among the clusters given in Table I, $Mn_{12}B_6$ has the smallest HOMO-LUMO gap, partly because B is not as electronegative as N. Although C is not as electronegative as N, $Mn_{12}C_6$ has a comparable HOMO-LUMO gap to that of $Mn_{12}N_6$. This is because one can think of $Mn_{12}C_6$ being composed of six Mn_2C units. Since every Mn_2C unit has 18 valence electrons, it forms a stable building block of $Mn_{12}C_6$. We found the ground state of Mn_2C cluster to be ferromagnetic with a magnetic moment of 8 μ_B and a large HOMO-LUMO gap of 1.2 eV; its geometric structure is almost an right angle triangle (as displayed in Fig. S4 of the supplementary material,[41] the Mn-C-Mn angle is 91.9°). This matches well with the geometry of $Mn_{12}C_6$ where each C atom resides at the center of square faces.

TABLE I. The HOMO-LUMO gap Δ, the average charge on the Mn (Q_M) and the doped atom (Q_d), the average Mn-Mn bond length, the total magnetic moment (Mt), and the average value of local magnetic moment of Mn (Ma).

	Δ (eV)	Q_M (e)	Q_d (e)	D_{MM} (Å)	Mt (μ_B)	Ma (μ_B)
$Mn_{12}B_6$	0.17	0.100	−0.20	2.68	16	3.35
$Mn_{12}C_6$	0.30	0.126	−0.252	2.60	38	3.23
$Mn_{12}N_6$	0.33	0.145	−0.290	2.52	0.0	3.25

The charge from Mn is transferred to the dopants and it is the largest for $Mn_{12}N_6$ and gradually decreases in $Mn_{12}C_6$ and $Mn_{12}B_6$. This is consistent with the electronegativity sequence of N>C>B discussed earlier. We also examined the interatomic distances in these clusters to clarify the origin of their different magnetic behavior. It has been reported previously that reduction in Mn-Mn distance results in a transition from ferromagnetic to antiferromagnetic ordering in Mn_2 dimer.[27] Note also that in Ref. 31, the Mn-Mn bond length in $[Mn_{13}@Au_{20}]^-$ with a magnetic moment of 44 μ_B is ∼9% larger than that in the bare Mn_{13}^- which has a moment of only 2 μ_B. In Table I, we find the Mn-Mn bond lengths $d(Mn_{12}C_6)>d(Mn_{12}N_6)$, which may explain why the hollow cage of $Mn_{12}C_6$ is ferromagnetic while $Mn_{12}N_6$ is antiferromagnetic. If we allow the cluster size to expand or contract uniformly without changing its symmetry as shown in the supplementary material (see Fig. S5),[41] the antiferromagnetic state of $Mn_{12}C_6$ becomes more favorable upon contraction, while the ferromagnetic state of $Mn_{12}N_6$ becomes more favorable upon expansion. In $Mn_{12}B_6$, as shown in Fig. 1(a), the Mn-Mn bond lengths between ferromagnetically coupled Mn atoms (colored green) are larger (around 2.75 Å) than the bond lengths between antiferromagnetically coupled Mn atoms (around 2.5 Å). In $Mn_{12}C_6$, the Mn-C bond is partly covalent and partly ionic. If the bonds were purely ionic, every Mn^{2+} ion should have a d^5 electron configuration and a magnetic moment of 5 μ_B. However, the calculated magnetic moment per Mn atom is 3.23 μ_B. As seen from the deformation density distribution in Fig. 3(d), electron density is delocalized between every C atom as well as its surrounding four Mn atoms, suggesting that the electronic structure is partially covalent.

To see if hollow cage structures can be obtained by replacing the Mn atoms in $Mn_{12}C_6$ by some other transition metal atoms, we replaced Mn by the first-row transition metal elements. We find that $M_{12}C_6$ clusters (M = Mn, Co, Ni, and Cu) prefer to form hollow cage structures (Fig. 5(a)) while for similar clusters with M = Sc, Ti, V, Cr, and Fe, the geometries are filled structures. In Fig. 5(a), M stands for all the late transition-metal elements except Mn. Among these clusters $Co_{12}C_6$ is the only one that is ferromagnetic, but carries a small magnetic moment of 14 μ_B. $Ni_{12}C_6$ and $Cu_{12}C_6$ are nonmagnetic. Here we find that $Ni_{12}C_6$ has an anomalously large HOMO-LUMO gap of 0.73 eV which is much larger than $Co_{12}C_6$'s 0.17 eVgap and $Cu_{12}C_6$'s 0.20 eV gap. We also studied Pd and Pt based clusters in the same group. $Pd_{12}C_6$ and $Pt_{12}C_6$ are found to have even larger HOMO-LUMO gaps

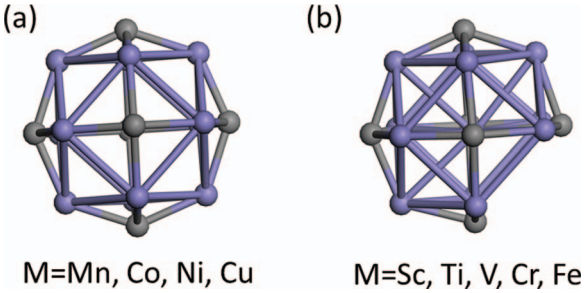

FIG. 5. (a) Hollow and (b) filled structures of $M_{12}C_6$ (M = Sc, Ti, V, Cr, Mn, Fe, Co, Ni, Cu) clusters.

of 0.85 and 0.90 eV, respectively. The large HOMO-LUMO gap of Ni originates from its electronic atomic configuration of $4s^2\ 3d^8$. In $Ni_{12}C_6$, Ni forms covalent bonds with C atom which has four valence electrons to share with two Ni atoms. As a result every Ni atom can form a closed shell configuration of $4s^2\ 3d^{10}$.

In a similar vein, $Cu_{12}O_6$ can also form a closed shell configuration. Here each Cu atom can donate one electron and Cu_2O with a closed shell configuration can form the building blocks of $Cu_{12}O_6$ which is found to have a large HOMO-LUMO gap of 1.3 eV. Stable electronic configuration can also be expected if we choose alkali metal elements such as Li. $Li_{12}O_6$ where Li_2O serves as the building block, is found to have the largest HOMO-LUMO gap of 2.8 eV. Similarly, $Ag_{12}O_6$, $Ag_{12}S_6$, $Au_{12}O_6$, and $Au_{12}S_6$ also have large HOMO-LUMO gaps of 2.2, 2.7, 1.0, and 2.5 eV, respectively.

Next we studied another type of large hollow cage cluster with dodecahedral symmetry that contains 20 vertices and 12 regular pentagonal faces. To see if a hollow cage can be formed we placed Mn atoms on the vertices and dopants in the center of pentagonal faces. In a Mn pentagon, if the edge Mn-Mn bond length is around 2.5∼2.8 Å, the distance from the center of the pentagon to a Mn atom should range from to 2.1 to 2.4 Å. Since this is larger than the C-Mn bond of about 2.0 Å, a carbon atom placed at the center may not yield a stable structure. Hence, we considered placing Si atoms at the center of the 12 pentagons since the bond length of Si-Mn is around 2.4 Å. This led to a $Mn_{20}Si_{12}$ cluster whose optimized structure is shown in Fig. 4(b). This cluster is dynamically stable with the lowest vibrational frequency of 62.9 cm^{-1}. $Mn_{20}Si_{12}$ cluster is found to be ferrimagnetic with a magnetic moment of 36 μ_B. The Mn-Mn bond length between ferromagnetic-coupled Mn atoms is around 2.68 Å, while that between antiferromagnetically coupled Mn atoms is 2.52 Å. In Fig. 4(c), we plot the relative energies of $Mn_{20}Si_{12}$ for different spin states measured with respect to the ground state, using the VASP code. It too yields a magnetic moment of 36 μ_B in the ground state. The binding energy with respect to dissociation of $Mn_{20}Si_{12}$ into Mn_{20} and Si_{12} cluster is 16.9 eV. We also checked another isomer of $Mn_{20}Si_{12}$ based on the optimized structure of a compact ground-state Mn_{20} cluster covered with 12 Si atoms. This isomer is 0.81 eV higher in energy, as shown in Fig. S2(f).[41] Finally, we replaced the C atoms in $Mn_{24}C_{18}$ in Fig. 4(a) by Si atoms. However, the resulting $Mn_{24}Si_{18}$ geometry, after optimization, becomes a compact structure instead of hollow cage, as shown in Fig. S2(g) of supplementary material.[41]

CONCLUSIONS

In summary, we have studied a series of metal-based cage clusters composed of transition metal atoms (Sc, Ti, V, Cr, Mn, Fe, Co, Ni, Cu, Pd, and Pt) stabilized by dopant atoms such as C, B, N, O, and Si. We find that $Mn_{12}C_6$ forms a ferromagnetic cuboctahedral hollow cage structure with a magnetic moment of 38 μ_B. A larger rhombicuboctahedral $Mn_{24}C_{18}$ cluster also forms a ferromagnetic hollow cage structure, but with a substantially higher magnetic moment of 70 μ_B. Replacement of Mn with other transition metal atoms and C with B, N, Si, and O have significant effects on their structure and magnetic properties due to changes in the Mn-Mn bonds: $Mn_{12}N_6$ is predicted to be an antiferromagnetic hollow cage, while $Mn_{12}B_6$ forms a compact ferrimagnetic structure. Other clusters like $Co_{12}C_6$, $Ni_{12}C_6$, $Cu_{12}C_6$, $Pd_{12}C_6$, $Cu_{12}O_6$, and $Li_{12}O_6$ are also found to have hollow cage configurations among which $Co_{12}C_6$ is the only cluster that is ferromagnetic, albeit with a reduced magnetic moment of 14 μ_B. $Ni_{12}C_6$, $Pd_{12}C_6$, $Cu_{12}O_6$, and $Li_{12}O_6$ have large HOMO-LUMO gaps because of closed-shell configurations. Dodecahedral $Mn_{20}Si_{12}$ cluster is ferrimagnetic with a magnetic moment of 36 μ_B. These studies based on density functional theory suggest that metal-based hollow cages can be formed and depending upon their composition, some of them can even carry very large magnetic moments. The space inside some of these hollow cage clusters is large enough to accommodate additional atoms or molecules raising the possibility that they may have technological applications. Besides, the surface dopant may act as ligands that are commonly present during chemical synthesis to protect the pure metal cluster, rendering their potential use as molecular magnets in spintronics applications.[43,44] We hope that these results will stimulate experimental efforts in the search for hollow metallic cages carrying large magnetic moments.

ACKNOWLEDGMENTS

This work is partly funded by a grant from the Department of Energy. We thank NSERC for computational resources.

[1]H. W. Kroto, J. R. Heath, S. C. O'Brien, R. F. Curl, and R. E. Smalley, Nature (London) **318**, 162 (1985).
[2]B. C. Guo, K. P. Kerns, and A. W. Castleman, Jr., Science **255**, 1411 (1992).
[3]B. C. Guo, S. Wei, J. Purnell, S. Buzza, and A. W. Castleman, Jr., Science **256**, 515 (1992).
[4]M. M. Rohmer, M. Benard, and J. M. Poblet, Chem. Rev. **100**, 495 (2000).
[5]L. Lou, T. Guo, P. Nordlander, and R. E. Smalley, J. Chem. Phys. **99**(7), 5301 (1993).
[6]B. Reddy, S. Khanna, and P. Jena, Science **258**, 1640 (1992).
[7]D. Heijinsbergen *et al.*, Phys. Rev. Lett. **83**, 4983 (1999).
[8]F. Tast *et al.*, Phys. Rev. Lett. **77**, 3529 (1996).
[9]D. Heijinsbergen, A. Fielicke, G. Meijer, and G. Helden, Phys. Rev. Lett. **89**, 013401 (2002).
[10]G. K. Gueorguiev and J. M. Pacheco, Phys. Rev. Lett. **88**, 115504 (2002).
[11]M. A. Sobhy, A. W. Castleman, and J. O. Sofo, J. Chem. Phys. **123**, 154106 (2005).

[12]T. Baruah, M. R. Pederson, M. L. Lyn, and A. W. Castleman, Jr., Phys. Rev. A **66**, 0553201 (2002).
[13]L. F. Cui, X. Huang, L. M. Wang, D. Y. Zubarev, A. I. Boldyrev, J. Li, and L. S. Wang, J. Am. Chem. Soc. **128**, 8390 (2006).
[14]L. F. Cui, X. Huang, L. M. Wang, J. Li, and L. S. Wang, J. Phys. Chem. A. **110**, 10169 (2006).
[15]S. Bulusu, X. Li, L. S. Wang, and X. C. Zeng, Proc. Natl. Acad. Sci. U.S.A. **103**, 8326 (2006).
[16]K. R. Asmis, G. Santambrogio, M. Brummer, and J. Sauer, Angew. Chem. Int. Ed. **44**, 3122 (2005).
[17]R. Fournier and S. A. Hussain, J. Chem. Phys. **138**, 054303 (2013).
[18]S. K. Nayak and P. Jena, Chem. Phys. Lett. **289**, 473 (1998).
[19]S. K. Nayak, B. K. Rao, and P. Jena, J. Phys. Condens. Matter **10**, 10863 (1998).
[20]P. Bobadova-Parvanova, K. A. Jackson, S. Srinivas, and M. J. Horoi, J. Chem. Phys. **122**, 014310 (2005).
[21]M. B. Knickelbein, Phys. Rev. Lett. **86**, 5255 (2001).
[22]M. B. Knickelbein, Phys. Rev. B **70**, 014424 (2004).
[23]T. M. Briere, M. H. F. Sluiter, V. Kumar, and Y. Kawzaoe, Phys. Rev. B **66**, 064412 (2002).
[24]M. Kabir, A. Mookerjee, and D. G. Kanhere, Phys. Rev. B **73**, 224439 (2006).
[25]S. N. Khanna, B. K. Rao, P. Jena, and M. Knickelbein, Chem. Phys. Lett. **378**, 374 (2003).
[26]M. J. Piotrowski, P. Piquini and J. L. F. Da Silva, Phys. Rev. B **81**, 155446 (2010).
[27]J. Mejia-Lopez, A. H. Romero, M. E. Garcia, and J. L. Moran-Lopez, Phys. Rev. B **78**, 134405 (2008).
[28]B. K. Rao and P. Jena, Phys. Rev. Lett. **89**, 185504 (2002).
[29]S. Datta, M. Kabir, A. Mookerjee, and T. S. Dasgupta, Phys. Rev. B **83**, 075425 (2011).
[30]M. Wu and P. Jena, Nanoscale **5**, 2114 (2013).
[31]J. Wang, J. Bai, J. Jellinek, and X. C. Zeng, J. Am. Chem. Soc. **129**(14), 4110 (2007).
[32]B. Delley, J. Chem. Phys. **92**, 508 (1990).
[33]B. Delley, J. Chem. Phys. **113**, 7756 (2000).
[34]J. P. Perdew, K. Burke, and M. Ernzerhof, Phys. Rev. Lett. **77**, 3865 (1996).
[35]M. Wu, A. K. Kandalam, G. L. Gutsev, and P. Jena, Phys. Rev. B **86**, 174410 (2012).
[36]P. E. Blöchl, Phys. Rev. B **50**, 17953 (1994).
[37]G. Kresse and D. Joubert, Phys. Rev. B **59**, 1758 (1999).
[38]G. Kresse and J. Hafner, Phys. Rev. B **47**: 558 (1993).
[39]G. Kresse and J. Hafner, Phys. Rev. B **49**, 14251 (1994).
[40]G. Kresse and J. Furthmuller, Phys. Rev. B **54**, 11169 (1996).
[41]See supplementary material at http://dx.doi.org/10.1063/1.4813022 for isomers of manganese compound clusters with different geometrical or spin structures.
[42]M. Yang, K. A. Jackson, and J. Jellinek, J. Chem. Phys. **125**, 144308 (2006).
[43]S. Barraza-Lopez, K. Park, V. Garcia-Suarez, and J. Ferrer, Phys. Rev. Lett. **102**, 206801 (2009).
[44]M. Zhou, Y. Q. Cai, M. G. Zeng, C. Zhang, and Y. P. Zhang, Appl. Phys. Lett. **98**, 143103 (2011).